

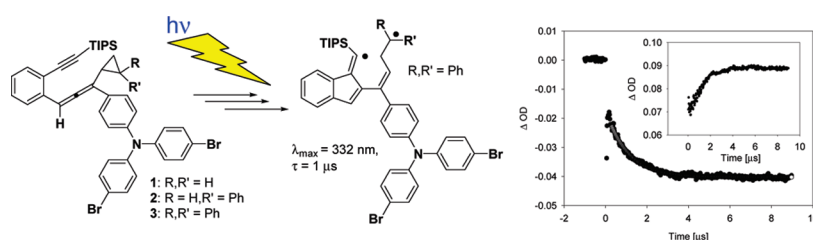
The Photochemical C²–C⁶ Cyclization of Enyne–Allenes: Interception of the Fulvene Diradical with a Radical Clock Ring Opening

Götz Bucher,^{*,†,§} Atul A. Mahajan,[‡] and Michael Schmittel^{*,‡}

[†]Lehrstuhl für Organische Chemie II, Ruhr-Universität Bochum, Universitätsstrasse 150, D-44801 Bochum, Germany, and [‡]Organische Chemie I, FB 8 (Chemie-Biologie), Universität Siegen, Adolf-Reichwein-Strasse, D-57068 Siegen, Germany. [§]Present address: WestCHEM, University of Glasgow, Joseph-Black-Building, University Avenue, Glasgow G12 8QQ, United Kingdom.

goebu@chem.gla.ac.uk; schmittel@chemie.uni-siegen.de

Received February 26, 2009



The mechanism of the photochemical C²–C⁶ cyclization of enyne–allenenes has been studied through radical clock, intramolecular kinetic isotope effect, and laser flash photolysis (LFP) experiments as well as density functional theory (DFT) and ab initio computations. While the photochemical cyclization of enyne–allenenes **1** and **2** furnished ene and Diels–Alder products without any cyclopropyl ring opening, that of **3** carrying the ultrafast diphenylcyclopropylcarbinyl radical clock afforded products derived from cyclopropyl ring opening. Laser flash photolysis (LFP) studies on enyne–allene **3** point to an allene triplet excited state (transient A) as a primarily formed short-lived ($\tau = 430 \text{ ns}$) intermediate. In addition, we have obtained evidence for the formation of a diphenylmethyl-type diradical (transient C, $\tau = 1.0 \mu\text{s}$) resulting from ring opening of a diphenylcyclopropane ring. C subsequently undergoes a surprisingly slow ($\tau = 1.0 \mu\text{s}$) 1,6-hydrogen shift leading to the stable 1,3-diene **6**.

Introduction

Natural enediyne antitumor antibiotics, such as neocarzinostatin, dynemicin, etc., avail themselves of two thermally

triggered diradical cyclizations, i.e., the Bergman¹ and Myers–Saito² cycloaromatizations, to ultimately damage DNA by hydrogen atom abstraction. Not surprisingly, the photochemical analogues of the Bergman³ and recently of the Myers–Saito⁴ cyclization have become equally a major concern of research due to their high applicability in photodynamic therapy (PDT).⁵ Along with the photochemical Myers–Saito (C²–C⁷) cycloaromatization, the photochemical C²–C⁶ cyclization of enyne–allenenes was observed as well.⁴ Apparently, spin control allows management between the two photochemical pathways, as the Myers–Saito (C²–C⁷) cycloaromatization was observed from the singlet mani-

(1) Bergman, R. G. *Acc. Chem. Res.* **1973**, *6*, 25–31.
(2) (a) Myers, A. G.; Kuo, E. Y.; Finney, N. S. *J. Am. Chem. Soc.* **1989**, *111*, 8057–8059. (b) Nagata, R.; Yamanaka, H.; Okazaki, E.; Saito, I. *Tetrahedron Lett.* **1989**, *30*, 4995–4998. (c) Saito, K.; Watanabe, T.; Takahashi, K. *Chem. Lett.* **1989**, 2099–2102. (d) Myers, A. G.; Dragovich, P. S.; Kuo, E. Y. *J. Am. Chem. Soc.* **1992**, *114*, 9369–9386.
(3) (a) Turro, N. J.; Evenzahav, A.; Nicolaou, K. C. *Tetrahedron Lett.* **1994**, *35*, 8089–8092. (b) Funk, R. L.; Young, E. R. R.; Williams, R. M.; Flanagan, M. F.; Cecil, T. L. *J. Am. Chem. Soc.* **1996**, *118*, 3291–3292. (c) Evenzahav, A.; Turro, N. J. *Am. Chem. Soc.* **1998**, *120*, 1835–1841. (d) Kaneko, T.; Takahashi, M.; Hiram, M. *Angew. Chem., Int. Ed.* **1999**, *38*, 1267–1268. (e) Choy, N.; Blanco, B.; Wen, J. H.; Krishan, A.; Russell, K. C. *Org. Lett.* **2000**, *2*, 3761–3764. (f) Clark, A. E.; Davidson, E. R.; Zaleski, J. M. *J. Am. Chem. Soc.* **2001**, *123*, 2650–2657. (g) Chandra, T.; Kraft, B. J.; Huffman, J. C.; Zaleski, J. M. *Inorg. Chem.* **2003**, *42*, 5158–5172. (h) Benites, P. J.; Holmberg, R. C.; Rawat, D. S.; Kraft, B. J.; Klein, L. J.; Peters, D. G.; Thorp, H. H.; Zaleski, J. M. *J. Am. Chem. Soc.* **2003**, *125*, 6434–6446. (i) Alabugin, I. V.; Manoharan, M. *J. Phys. Chem. A* **2003**, *107*, 3363–3371.

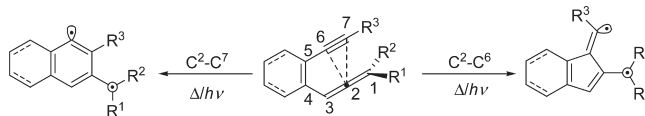
(4) Schmittel, M.; Mahajan, A. A.; Bucher, G. *J. Am. Chem. Soc.* **2005**, *127*, 5324–5325.

(5) (a) Boyle, R. W.; Dolphin, D. *Photochem. Photobiol.* **1996**, *64*, 469–485. (b) Ali, H.; van Lier, J. E. *Chem. Rev.* **1999**, *99*, 2379–2450. (c) Ackroyd, R.; Kilty, C.; Brown, N.; Reed, M. *Photochem. Photobiol.* **2001**, *74*, 656–669. (d) Bonnett, R.; Martinez, G. *Tetrahedron* **2001**, *57*, 9513–9547.

fold, whereas the photochemical C^2-C^6 cyclization could be ignited after triplet excitation (Scheme 1). On the basis of a combined LFP and DFT study, it was recently suggested that the photochemical C^2-C^6 cyclization evolves from a triplet allene intermediate ($\tau = 30$ ns) that initiates benzofulvene formation.⁶ In contrast, the exact nature of the long-lived intermediate ($\tau = 30 \mu\text{s}$) was not identified beyond doubt, although experimental and computational evidence pointed to a fulvene triplet diradical. As the thermal C^2-C^6 cyclization of enyne-allenes has become important over the past decade due to its striking potential for the synthesis of complex carbocycles⁷ and for DNA cleavage,⁸ a mechanistic comparison of the thermal and photochemical diradical cyclization pathways should open further venues for the synthetic use of enyne-allenes.

The thermal C^2-C^6 cyclization of enyne-allenes has been extensively studied over the past few years, both mechanistically⁹ and computationally.¹⁰ Some years back, our group as well as Lipton et al. investigated the C^2-C^6 cyclization using radical clock experiments, but all early attempts to locate cyclopropyl ring-opened products in the thermal C^2-C^6 cyclization of enyne-allenes were met with failure.^{9a,11} Cyclopropyl¹² substrates have been successfully

SCHEME 1. Thermal and Photochemical Myers–Saito (C^2-C^7) and C^2-C^6 Cyclizations of Enyne–Allenes



used as a kinetic clock¹³ and as a mechanistic probe¹⁴ for radical and diradical^{15,16} intermediates. Formation of ring-opened products via the cyclopropylcarbinyl substrate is generally accepted as evidence for the formation of a radical intermediate. Very recently, we have disclosed experimental evidence for the stepwise mechanism in the thermal C^2-C^6 cyclization of enyne-allenes using an ultrafast radical clock.¹⁷ Encouraged by this finding, we decided to interrogate also the photochemical route using the radical clock as a mechanistic probe and to complement these studies with kinetic isotope and laser flash photolysis investigations to further understand the nature of the long-lived intermediate.

Results

As part of our study to comprehend the mechanism of the photochemical C^2-C^6 cyclization, we have chosen enyne-allenes **1–3** (Chart 1) as model compounds due to their special features: (1) the trisopropylsilanyl group (TIPS) at the alkyne terminus raises the cyclization barrier thus precluding any thermal reaction during photolysis; (2) the bis-(4-bromophenyl)amine unit was used as an internal triplet sensitizer to initiate the photochemical reaction; and (3) the “radical clock” reporter group was attached to the allene terminus to trap the radical intermediate.

Synthesis. Preparation of enyne-allenes **1–3** is described elsewhere.¹⁷ **4** was obtained in a three-step synthesis from benzaldehyde after addition of $\text{BrMgC}\equiv\text{C}-\text{R}$, (prepared from the reaction of EtMgBr with $\text{R} = 1\text{-ethynyl-2,2-diphenylcyclopropane}^{18}$), acetylation of the propargyl alcohol with acetic anhydride/DMAP, and concluding with

(6) Bucher, G.; Mahajan, A. A.; Schmittel, M. *J. Org. Chem.* **2008**, *73*, 8815–8828.

(7) (a) Zhang, H. R.; Wang, K. K. *J. Org. Chem.* **1999**, *64*, 7996–7999. (b) Wang, K. K.; Zhang, H. R.; Petersen, J. L. *J. Org. Chem.* **1999**, *64*, 1650–1656. (c) Yang, Y. H.; Petersen, J. L.; Wang, K. K. *J. Org. Chem.* **2003**, *68*, 5832–5837. (d) Yang, Y. H.; Petersen, J. L.; Wang, K. K. *J. Org. Chem.* **2003**, *68*, 8545–8549.

(8) (a) Schmittel, M.; Kiau, S.; Siebert, T.; Strittmatter, M. *Tetrahedron Lett.* **1996**, *37*, 7691–7694. (b) Schmittel, M.; Maywald, M.; Strittmatter, M. *Synlett* **1997**, 165–166.

(9) (a) Schmittel, M.; Strittmatter, M.; Kiau, S. *Angew. Chem., Int. Ed. Engl.* **1996**, *35*, 1843–1845. (b) Schmittel, M.; Strittmatter, M.; Vollmann, K.; Kiau, S. *Tetrahedron Lett.* **1996**, *37*, 999–1002. (c) Schmittel, M.; Steffen, J. P.; Auer, D.; Maywald, M. *Tetrahedron Lett.* **1997**, *38*, 6177–6180. (d) Schmittel, M.; Keller, M.; Kiau, S.; Strittmatter, M. *Chem.—Eur. J.* **1997**, *3*, 807–816. (e) Engels, B.; Lennartz, C.; Hanrath, M.; Schmittel, M.; Strittmatter, M. *Angew. Chem., Int. Ed.* **1998**, *37*, 1960–1963. (f) Schmittel, M.; Strittmatter, M. *Tetrahedron* **1998**, *54*, 13751–13760. (g) Li, H. B.; Zhang, H. R.; Petersen, J. L.; Wang, K. K. *J. Org. Chem.* **2001**, *66*, 6662–6668. (h) Schmittel, M.; Steffen, J. P.; Maywald, M.; Engels, B.; Helten, H.; Musch, P. *J. Chem. Soc., Perkin Trans. 2* **2001**, 1331–1339. (i) Yang, Y. H.; Petersen, J. L.; Wang, K. K. *J. Org. Chem.* **2003**, *68*, 5832–5837. (j) Yang, Y. H.; Petersen, J. L.; Wang, K. K. *J. Org. Chem.* **2003**, *68*, 8545–8549.

(10) (a) Engels, B.; Hanrath, M. *J. Am. Chem. Soc.* **1998**, *120*, 6356–6361. (b) Schreiner, P. R.; Prall, M. *J. Am. Chem. Soc.* **1999**, *121*, 8615–8627. (c) Cramer, C. J.; Kormos, B. L.; Seierstad, M.; Sherer, E. C.; Winget, P. *Org. Lett.* **2001**, *3*, 1881–1884. (d) de Visser, S. P.; Filatov, M.; Shaik, S. *Phys. Chem. Chem. Phys.* **2001**, *3*, 1242–1245. (e) Stahl, F.; Moran, D.; Schleyer, P. V.; Prall, M.; Schreiner, P. R. *J. Org. Chem.* **2002**, *67*, 1453–1461. (f) Schreiner, P. R.; Navarro-Vazquez, A.; Prall, M. *Acc. Chem. Res.* **2005**, *38*, 29–37.

(11) Brunette, S. R.; Lipton, M. A. *J. Org. Chem.* **2000**, *65*, 5114–5119.

(12) (a) Shimizu, N.; Nishida, S. *J. Chem. Soc., Chem. Commun.* **1972**, 389–390. (b) Rudolph, A.; Weedon, A. C. *Can. J. Chem.* **1990**, *68*, 1590–1596. (c) Newcomb, M.; Johnson, C. C.; Manek, M. B.; Varick, T. R. *J. Am. Chem. Soc.* **1992**, *114*, 10915–10921. (d) Adam, W.; Curci, R.; D’Accolti, L.; Dinoi, A.; Fusco, C.; Gasparrini, F.; Kluge, R.; Paredes, R.; Schulz, M.; Smerz, A. K.; Veloza, L. A.; Weinköt, S.; Winde, R. *Chem.—Eur. J.* **1997**, *3*, 105–109.

(13) (a) Griller, D.; Ingold, K. U. *Acc. Chem. Res.* **1980**, *13*, 317–323. (b) Engel, P. S.; Keys, D. E. *J. Am. Chem. Soc.* **1982**, *104*, 6860–6861. (c) Campredon, M.; Kanabus-Kaminska, J. M.; Griller, D. *J. Org. Chem.* **1988**, *53*, 5393–5396. (d) Castellino, A. J.; Bruice, T. C. *J. Am. Chem. Soc.* **1988**, *110*, 1313–1315. (e) Newcomb, M.; Manek, M. B.; Glenn, A. G. *J. Am. Chem. Soc.* **1991**, *113*, 949–958. (f) Adam, W.; Heil, M. *J. Am. Chem. Soc.* **1991**, *113*, 1730–1736. (g) Adam, W.; Finzel, R. *J. Am. Chem. Soc.* **1992**, *114*, 4563–4568. (h) Newcomb, M. *Tetrahedron* **1993**, *49*, 1151–1176. (i) Engel, P. S.; Wu, A. Y. *J. Org. Chem.* **1994**, *59*, 3969–3974. (j) Caldwell, R. A.; Zhou, L. W. *J. Am. Chem. Soc.* **1994**, *116*, 2271–2275. (k) Engel, P. S.; Lowe, K. L. *Tetrahedron Lett.* **1994**, *35*, 2267–2270. (l) Tanko, J. M.; Blackert, J. F. *J. Chem. Soc., Perkin Trans. 2* **1996**, 1775–1779. (m) Cooksy, A. L.; King, H. F.; Richardson, W. H. *J. Org. Chem.* **2003**, *68*, 9441–9452.

(14) (a) Alonso, M. E.; Hernandez, M. I.; Gomez, M.; Jano, P.; Pekerar, S. *Tetrahedron* **1985**, *41*, 2347–2354. (b) Baldwin, J. E.; Adlington, R. M.; Domayne-Hayman, B. P.; Knight, G.; Ting, H.-H. *J. Chem. Soc., Chem. Commun.* **1987**, 1661–1663. (c) Suckling, C. J. *Angew. Chem., Int. Ed. Engl.* **1988**, *27*, 537–552. (d) Slama, J. T.; Satsangi, R. K.; Simmons, A.; Lynch, V.; Bolger, R. E.; Suttie, J. *J. Med. Chem.* **1990**, *33*, 824–832. (e) Arasasingham, R. D.; He, G.-X.; Bruce, T. C. *J. Am. Chem. Soc.* **1993**, *115*, 7985–7991. (f) Dixon, C. E.; Hughes, D. W.; Baines, K. M. *J. Am. Chem. Soc.* **1998**, *120*, 11049–11053. (g) Hartshorn, R. M.; Telfer, S. G. *J. Chem. Soc., Dalton Trans.* **1999**, 3565–3571. (h) Newcomb, M.; Toy, P. H. *Acc. Chem. Res.* **2000**, *33*, 449–455. (i) Kretzschmar, I.; Levinson, J. A.; Friend, C. M. *J. Am. Chem. Soc.* **2000**, *122*, 12395–12396. (j) Adam, W.; Roschmann, K. J.; Saha-Möller, C. R.; Seebach, D. *J. Am. Chem. Soc.* **2002**, *124*, 5068–5073. (k) Tokuyasu, T.; Kunikawa, S.; Masuyama, A.; Nojima, M. *Org. Lett.* **2002**, *4*, 3595–3598. (l) Samuel, M. S.; Baines, K. M. *J. Am. Chem. Soc.* **2003**, *125*, 12702–12703. (m) Samuel, M. S.; Jenkins, H. A.; Hughes, D. W.; Baines, K. M. *Organometallics* **2003**, *22*, 1603–1611. (n) Flemmig, B.; Kretzschmar, I.; Friend, C. M.; Hoffmann, R. *J. Phys. Chem. A* **2004**, *108*, 2972–2981. (o) Tong, X.; DiLabio, G. A.; Clarkin, O. J.; Wolkow, R. A. *Nano Lett.* **2004**, *4*, 357–360.

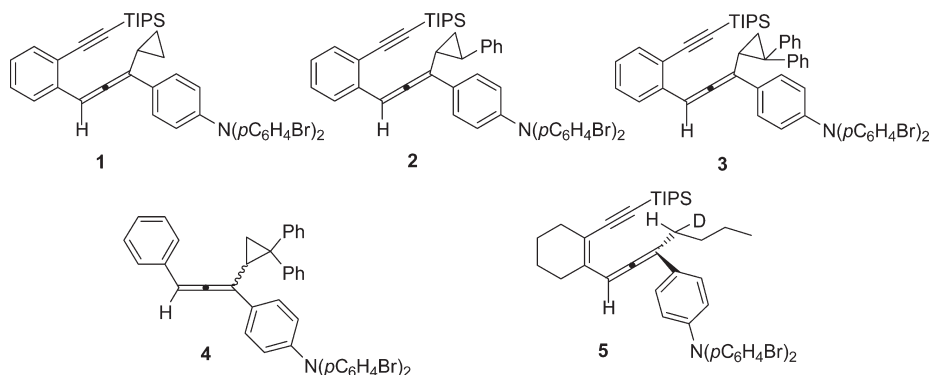
(15) (a) Wagner, P. J.; Liu, K.-C.; Noguchi, Y. *J. Am. Chem. Soc.* **1981**, *103*, 3837–3841. (b) Cheng, K.-L.; Wagner, P. J. *J. Am. Chem. Soc.* **1994**, *116*, 7945–7946. (c) Gan, C. Y.; Lambert, J. N. *J. Chem. Soc., Perkin Trans. 1* **1998**, 2363–2372. (d) Dopico, P. G.; Finn, M. G. *Tetrahedron* **1999**, *55*, 29–62. (e) Broyles, D. A.; Carpenter, B. K. *Org. Biomol. Chem.* **2005**, *3*, 1757–1767.

(16) For a theoretical study on radical clock openings see: Jäger, C. M.; Hennemann, M.; Mieszala, A.; Clark, T. *J. Org. Chem.* **2008**, *73*, 1536–1545.

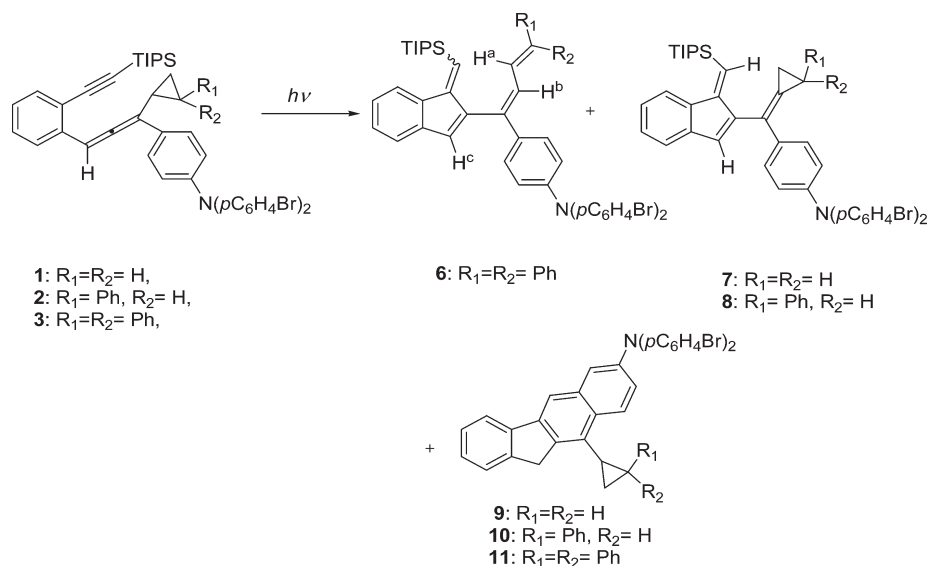
(17) Schmittel, M.; Mahajan, A. A.; Bucher, G.; Bats, J. W. *J. Org. Chem.* **2007**, *72*, 2166–2173.

(18) Bettinetti, G. F.; Desimoni, G.; Gruenanger, P. *Gazz. Chim. Ital.* **1964**, *94*, 91–108.

CHART 1. Model Compounds 1–5 Used in the Photochemical Investigation



SCHEME 2. Photochemical Cyclization of Enyne–Allenes 1–3



allene formation¹⁹ by introducing the triarylamine unit as $R'/ZnCl$ in the presence of $Pd(PPh_3)_4$. The monodeuterated enyne–allene **5** was prepared by using our established protocol^{20,21} by adding the deuterated butyl group as $CH_3CH_2CH_2CHD-MgBr$ in the presence of $CuI/LiBr$ ²² to the propargyl alcohol derivative in the last step (see the Supporting Information).

Photolysis. Photolysis of a 1.43 mM solution of **1** in toluene in the presence of an excess of 1,4-cyclohexadiene (1,4-CHD) at 300 nm in the Rayonet reactor afforded ene and formal Diels–Alder products **7** and **9**, each in 8% yield (Scheme 2; Table 1). The 1H and ^{13}C NMR spectra of **7** and **9** are in full agreement with those of formal ene and Diels–Alder products isolated from the thermal cyclization of enyne–allene **1**.¹⁷ Under analogous photolysis conditions, enyne–allene **2** provided the formal ene product **8**²³ along

with Diels–Alder product **10** in 8% and 12% yield, respectively. In contrast, photolysis of **3** in toluene (1.25 mM solution) afforded the cyclopropyl ring-opened product **6** in 40% yield (two isomers),^{24a} along with the formal Diels–Alder product **11**, isolated in 4% yield. The structure of compound **6** was assigned on the basis of 1H , ^{13}C , 1H , 1H -COSY, HSQC, and HRMS NMR data. The 1H NMR showed a characteristic doublet with a coupling constant ~ 11.6 Hz for the two olefinic protons H^a and H^b . Moreover, 1H , 1H -COSY clearly showed the coupling between H^a and H^b . A control experiment was carried out with **3** in toluene- d_8 . The lack of deuterium incorporation in **6** suggested that

(19) Elsevier, C. J.; Stehouwer, P. M.; Westmijze, H.; Vermeer, P. *J. Org. Chem.* **1983**, *48*, 1103–1105.

(20) Schmittel, M.; Vavilala, C. *J. Org. Chem.* **2005**, *70*, 4865–4868.

(21) Schmittel, M.; Vavilala, C.; Jaquet, R. *Angew. Chem., Int. Ed.* **2007**, *46*, 6911–6914.

(22) Macdonald, T. L.; Reagan, D. R.; Brinkmeyer, R. S. *J. Org. Chem.* **1980**, *45*, 4740–4747.

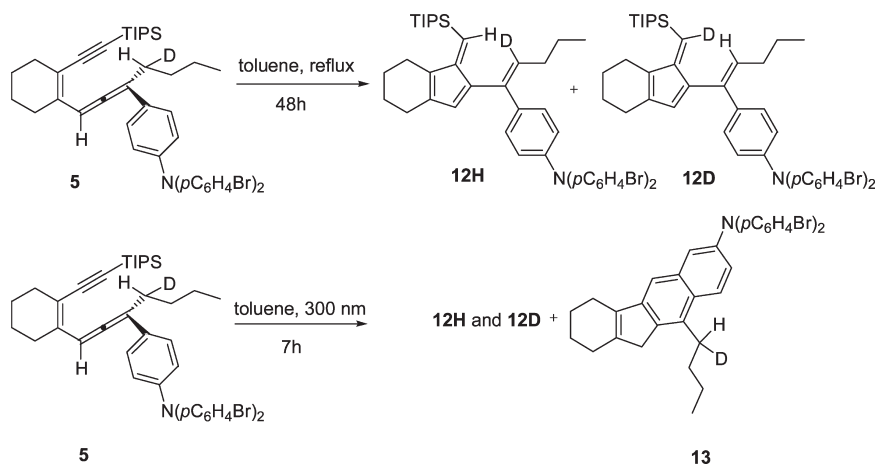
(23) The purification of ene product was difficult due to the unidentified impurities with the same R_f value.

(24) (a) The second isomer of **6** (isomer about the TIPS-C=C bond) arises from a follow-up irradiation of the photolabile product **6** as demonstrated by a photolysis of the thermally generated isomerically pure **6**. (b) Transient **C** shows up as negative absorption in the difference spectrum shown in Figure 2, but it can also be seen in Figure 1. At $\lambda=332$ nm, the transient decay of **C** is seen on top of a strong negative absorption due to bleaching of the precursor. The transient spectrum recorded 450 ns after LFP (solid circles) shows a less negative absorbance at $\lambda=332$ nm than the transient spectra recorded 1.7 or 7.5 μs after LFP (open circles and solid triangles). If the 450 ns spectrum is subtracted from the 7.5 μs spectrum (as in Figure 2), a less negative number is subtracted from a more negative number, resulting in a net negative absorption at $\lambda=332$ nm in Figure 2. By displaying the data in this format, the characteristic sharp band signature of the diphenylmethyl radical moiety is visualized, which is not easily seen from Figure 1 alone.

TABLE 1. Yields of C²–C⁶ Products after Irradiation of 1–3 at 300 nm

compd (conc)	λ_{\max} /nm (in hexane)	solvent (irradiation time)	ene product (yield) ^a	DA product ^b (yield) ^a
1 (1.43 mM)	206, 244, 267, 320	toluene + CHD ^c (6 h)	7 (8%)	9 (8%)
2 (1.40 mM)	212, 247, 262, 317	toluene + CHD ^c (7 h)	8 (8%)	10 (12%)
3 (1.25 mM)	212, 272, 322	toluene + CHD ^c (5 h)	6 (40%) ^d	11 (4%)

^aYield after isolation, estimated relative error 10%. ^bDA: formal Diels–Alder. ^cIn the presence of 1,4-cyclohexadiene (200-fold of excess). ^d[1,6]-H shift product.

SCHEME 3. Thermal and Photochemical Cyclization of Enyne–Allene 5**TABLE 2.** Intramolecular Kinetic Isotope Effect in the C²–C⁶ Photochemical and Thermal Cyclization of 5

reaction conditions	solvent (reaction time)	intramolecular KIE (d_1)	yield, %	
			ene products 12H, 12D ^a	DA ^b product 13 ^a
thermal	toluene (48 h)	1.0016 ^c	63	
photochemical	toluene (7 h)	1.0088 ^c	10	15

^aYield of isolated material, estimated relative error 10%. ^bDA: formal Diels–Alder. ^cEstimated error: $^{21} \pm 0.002$.

the hydrogen transfer proceeded in an intramolecular fashion, e.g., as sketched for C in Scheme 4.

Intramolecular Kinetic Isotope Effect. Recent investigations on thermal enyne–allene cyclizations have shown interesting signatures with regard to kinetic isotope effects,²¹ which we wanted to apply as a test for possibly identical intermediates in the thermal and photochemical cyclization. To evaluate the intramolecular kinetic isotope effect, the thermal cyclization of the monodeuterated enyne–allene **5** was investigated. It afforded a 1:1 mixture of the cyclized ene products **12H, 12D** in reasonable yield (63%), resulting in an intramolecular kinetic isotope effect of 1.0016 (at 110 °C). Upon photolysis of enyne–allene **5**, the formal ene **12H, 12D** (1:1) and Diels–Alder products **13** were isolated in 10% and 15% yield (Scheme 3; Table 2). Notably, the two ene products **12H, 12D** were formed with a comparable intramolecular kinetic isotope effect in both the thermal and photochemical reaction channel.

Laser Flash Photolysis. In the LFP experiment, excitation ($\lambda_{\text{exc}} = 355$ nm) of a solution of **3** in cyclohexane purged with argon led to the observation of three decaying transients A–C. Transients A and B were found to exhibit very similar

absorption maxima at λ_{\max} at ca. 458 nm (A: $k_A = (2.3 \pm 0.5) \times 10^6 \text{ s}^{-1}$; B: $k_B = (3.4 \pm 0.8) \times 10^5 \text{ s}^{-1}$). Transient C showed a $\lambda_{\max} = 332$ and ~ 500 nm ($k_C = (1.0 \pm 0.1) \times 10^6 \text{ s}^{-1}$, transient C is most easily seen as negative absorption in Figure 2).^{24b} In addition, we observed the growing transient D at $\lambda_{\max} = 380$ nm ($k = (1.0 \pm 0.1) \times 10^6 \text{ s}^{-1}$). A very weak transient absorption ($k_{\text{decay}} \approx 3.8 \times 10^5 \text{ s}^{-1}$) extending to $\lambda = 600$ nm also belongs to B. The fast component of the 458 nm transient, i.e., A ($\tau = 435$ ns), was quenched by $^3\text{O}_2$ at a diffusion controlled rate, $k_{A, \text{O}_2} = (4.7 \pm 0.7) \times 10^9 \text{ M}^{-1} \text{ s}^{-1}$. In contrast, the slow component of the 458 nm transient, i.e., B, showed no observable reactivity toward $^3\text{O}_2$. Transient C ($\lambda_{\max} = 332$ nm) decays with a lifetime $\tau = 1.0 \mu\text{s}$. It was quenched by $^3\text{O}_2$ at a near diffusion-controlled rate, $k_{C, \text{O}_2} = (1.2 \pm 0.2) \times 10^9 \text{ M}^{-1} \text{ s}^{-1}$. Concomitant with the decay of C we observed a growing transient at $\lambda_{\max} = 380$ nm. This species D was stable on the longest time scale (ca. 50 ms) accessible to our experimental setup. Apart from D, no transient growth was detectable in our experiments even on the shortest time scale accessible to our instrument (ca. 20 ns). Figure 1 shows the transient spectra observed during different time intervals after LFP of **3**, and Figure 2 shows a transient difference spectrum. Transient traces are given in Figures S1 and S2 in the SI.

For comparison, we also investigated an allene compound devoid of the alkyne moiety in the ortho position. LFP ($\lambda_{\text{exc}} = 355$ nm, cyclohexane solution) of **4** furnished a transient spectrum with $\lambda_{\max} = 430$ and 470 nm, and a transient lifetime $\tau = 1 \mu\text{s}$ (Figure 3). This transient was quenched by $^3\text{O}_2$ with a rate constant $k_{\text{O}_2} = (2.5 \pm 0.5) \times 10^9 \text{ M}^{-1} \text{ s}^{-1}$ (Figure S6, see the SI).

Discussion

Identity of the Transients As Derived from LFP. The LFP results of linear allene **4** show a short-lived transient ($\tau = 1 \mu\text{s}$)

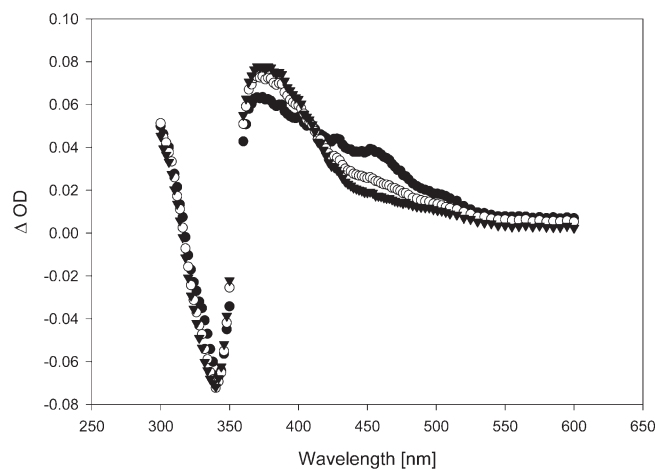


FIGURE 1. Transient spectra, observed during different time intervals after LFP (355 nm) of **3** in cyclohexane (1 atm of Ar): (solid circles) time window centered 450 ns after LFP; (open circles) time window centered 1.7 μ s after LFP; and (solid triangles) time window centered 7.5 μ s after LFP.

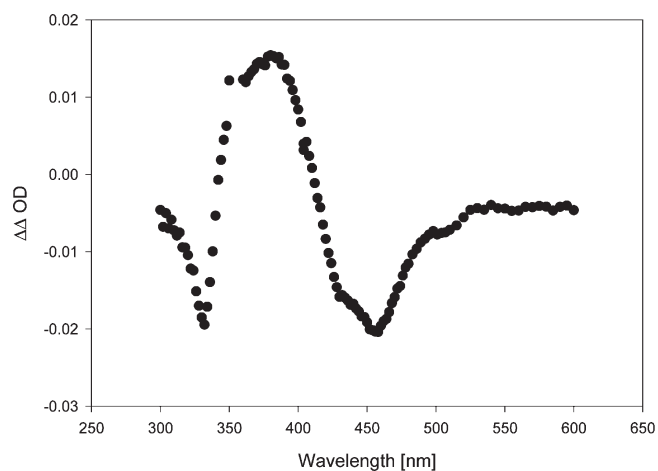


FIGURE 2. Transient difference spectrum derived from two of the transient spectra shown in Figure 1. The spectrum given here displays the difference between the 7.5 μ s and 450 ns time windows.

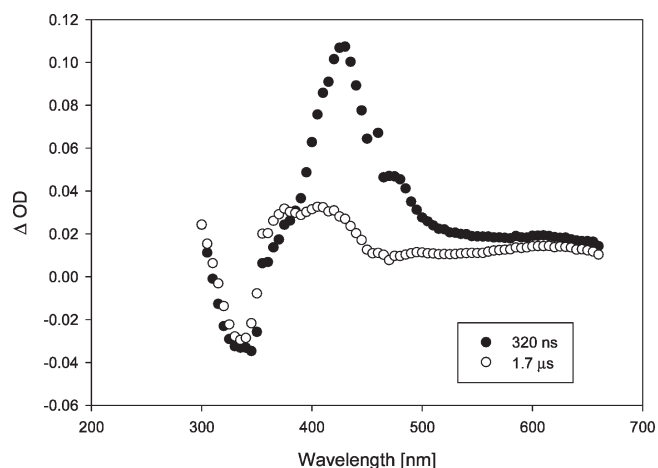


FIGURE 3. Transient spectra, observed during two different time intervals after LFP (355 nm, cyclohexane) of **4**: (solid circles) 320 ns after excitation and (open circles) 1.7 μ s after excitation.

with $\lambda_{\text{max}} = 430$ and 470 nm. A similar transient ($\lambda_{\text{max}} = 400$ nm, $\tau = 980$ ns) has recently been observed in the LFP and pulse radiolysis of 1,3-diphenylallene,²⁵ which was assigned to the first triplet excited state of 1,3-diphenylallene. Triplet tetraphenylallene ($\lambda_{\text{max}} = 385$ nm)²⁶ has been reported to have a shorter lifetime ($\tau = 90$ ns). On the basis of these results and the characteristic reactivity toward oxygen, we assign the transient species **A** (of **3**, Scheme 4) and the transient of **4** to a triplet excited state of the allene. Cyclopropyl ring opening at this stage is slow, as demonstrated also by preparative photochemical results: when allene **4** was subjected to photolysis at 300 nm in dry degassed toluene, no ring opening occurred and only starting material **4** was recovered.

Transient **B** could possibly be assigned to a fulvene–diyl diradical, either in its triplet or singlet spin multiplicity. Due to steric shielding of the reactive vinylic radical center by the bulky TIPS group, even a triplet fulvene–diyl may react rather slowly with oxygen⁶ and cannot be discarded as intermediate. As transient **C** shows a characteristic sharp absorption maximum at $\lambda_{\text{max}} = 332$ nm and additionally a high reactivity toward oxygen, we assign it to an intermediate containing a diphenylmethyl radical moiety (Scheme 4).²⁷ Notably, we do not observe such typical sharp absorption for the diphenylmethyl radical moiety ($\lambda_{\text{max}} = 332$ nm) in the LFP of linear allene **4**. Hence, we can reliably exclude formation of **C** directly from the allene triplet via intermediate **E**, suggesting that the cyclopropane ring opens at the diradical stage, either singlet or triplet (path 1). Transient **C** finally leads to the formation of transient **D**, which we assign to **6** as suggested by identical absorption maxima, i.e., $\lambda_{\text{max}} = 380$ nm, for both **D** and **6**.

At this point two important questions still remain unresolved. (i) What is the multiplicity of the fulvene–diyl diradical that we assign to transient **B**? (ii) Does the cyclopropylcarbinyl rearrangement take place at the singlet or triplet diradical stage? Experimentally, these questions are addressed in the following by DFT calculations as well as by radical clock and intramolecular kinetic isotope effects.

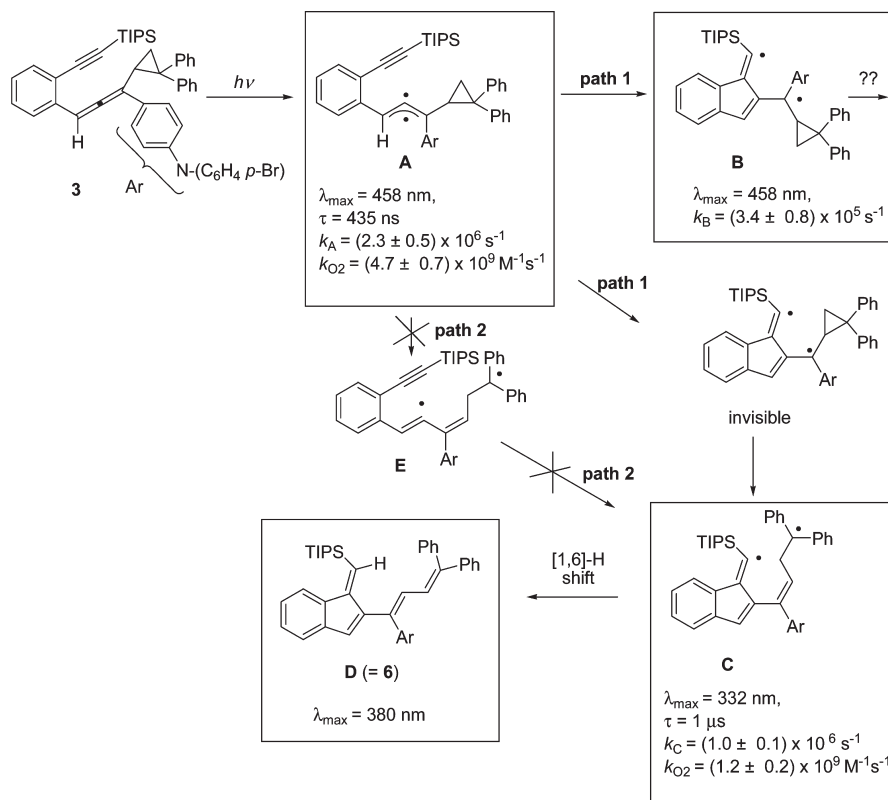
Calculations. We have performed a series of calculations on potential reaction intermediates formed upon photolysis of model compound **3'**. For this, we have employed a standard DFT method (B3LYP) in combination with a 6-31G(d) basis set. To facilitate the calculations on this sizable system to some degree, the remote bromine atom substituents in the experimentally studied system **3** were omitted in the calculations. Calculations on **3'** and the transients derived thereof are complicated by the fact that the molecular framework of **3/3'** in itself is chiral. In combination with the chiral diphenylcyclopropyl unit, two possible diastereomers (*l* and *u*) were received that in our hands could not be separated experimentally. Unfortunately, this complication also applies to many of the reaction intermediates to be discussed here, as most of them are also inherently chiral.

Precursor **3' and its triplet excited states:** The equilibrium geometries of two rotamers (*syn*, *anti*) of both diastereomers

(25) Yamashita, T.; Nishiguchi, T.; Kato, J.; Muroya, Y.; Katsumura, Y. *J. Photopolym. Sci. Technol.* **2005**, *18*, 95–102.

(26) Brennan, C. M.; Caldwell, R. A.; Elbert, J. E.; Unett, D. J. *J. Am. Chem. Soc.* **1994**, *116*, 3460–3464.

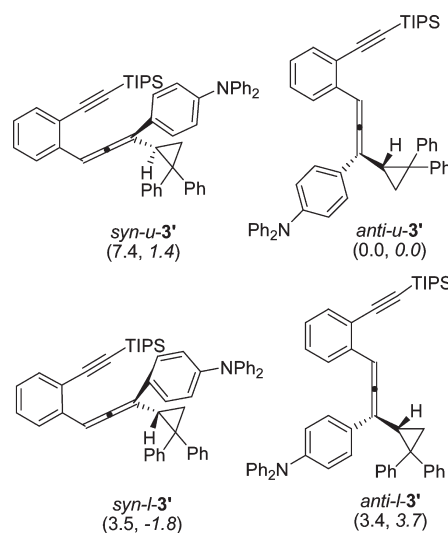
(27) (a) Hadel, L. M.; Platz, M. S.; Scaiano, J. C. *J. Am. Chem. Soc.* **1984**, *106*, 283–287. (b) Klett, M. W.; Johnson, R. P. *J. Am. Chem. Soc.* **1985**, *107*, 3963–3971.

SCHEME 4. Initial Hypothesis Assigning the Observed Transients to Possible Intermediates/Products^a

^aThe observed transients B and C are kinetically not linked to each other.

of **3'** (*u* and *l*) were localized. In the case of the *u*-diastereomer, the *anti*-rotamer is predicted to be the lowest energy conformer, being $7.4 \text{ kcal mol}^{-1}$ more stable than the *syn*-rotamer. The situation is different with the *l*-diastereomer. To our surprise, the *anti*-rotamer is predicted to be only $0.1 \text{ kcal mol}^{-1}$ more stable than the *syn*-rotamer. The calculations thus indicate that the *anti*-rotamer should be exclusively present in *u*-**3'**, while the *syn*- and *anti*-rotamers of *l*-**3'** should have roughly equal equilibrium concentrations. Scheme 5 shows the molecules and their energies (relative to *anti*-*u*-**3'** = $0.0 \text{ kcal mol}^{-1}$). On the basis of the geometries optimized at the B3LYP/6-31G(d) level of theory, we additionally calculated single-point energies at the RIMP2/TZVP level of theory, which should better describe the impact of weak intramolecular dispersive interactions.^{28a} The results of these ab initio calculations (also given in Scheme 5) indicate that the stability of the two *syn*-rotamers of **3'** is underestimated by DFT by $5\text{--}6 \text{ kcal mol}^{-1}$. Interestingly, for *l*-**3'** the *syn*-conformation is more stable than the *anti*-conformation by $5.5 \text{ kcal mol}^{-1}$!

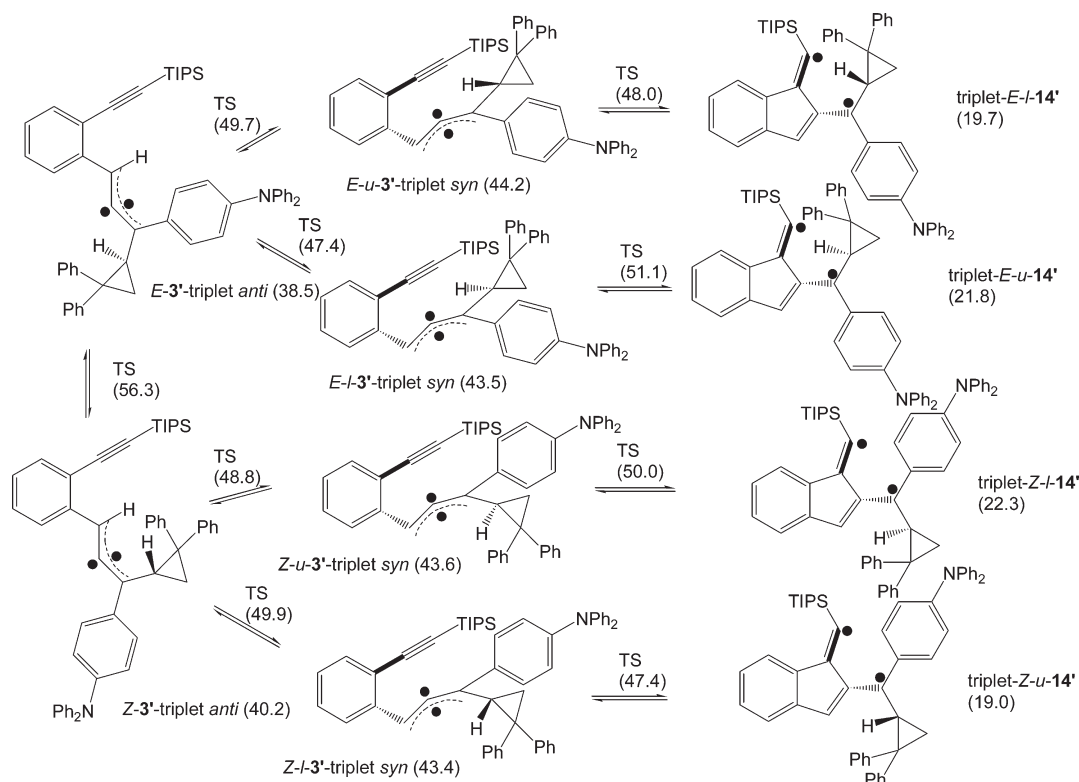
According to our calculations, the first triplet excited states of *l*-**3'** and *u*-**3'** are typical allene-type triplets with an allyl–vinyl type diradical character. The triplet states may contain up to four stereogenic elements, i.e., a stereogenic axis, twice *Z/E*-isomerism, and a stereogenic center in the diphenylcyclopropyl

SCHEME 5. Singlet Ground State Enthalpies of Isomers of **3'**, Relative to *anti*-*u*-**3'** = $0.0 \text{ kcal mol}^{-1}$ ^a

^aRegular font: B3LYP/6-31G(d), including ZPE correction. In italics: RIMP2/TZVP//B3LYP/6-31G(d), without ZPE correction.

group. Helicity arises in the *syn*-triplet states of **3'** along the allyl–vinyl-type diradical site due to an interaction of the bulky substituent (diphenylcyclopropyl or diphenylaminophenyl) forcing the phenylacetylene TIPS unit slightly out of the common plane. The energetically lower lying *anti*-conformers do not suffer this steric repulsion and are nearly planar.^{28b} Therefore, a total of 12 stereoisomeric triplet states consisting

(28) (a) Unlike MP2 theory, B3LYP will tend to underestimate weak dispersive interactions (cf.: Zhao, Y.; Tishchecko, O.; Truhlar, D. G. *J. Phys. Chem. B* **2005**, *109*, 19046–19051). This will result in enthalpies of the *syn*-rotamers that are too high, as in the case of the precursor ground states, see above. (b) We have not been able to extend the RIMP2 single-point calculations to the triplet hypersurface.

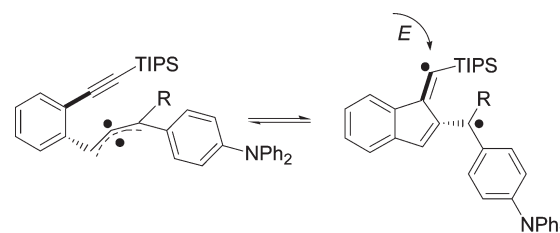
SCHEME 6. Reaction Pathways Leading from *anti*-Conformers of Triplet Excited States of **3'** to Triplet States of Fulvene–Diyl Diradicals **14'**^a

^aIn brackets: calculated enthalpies (in kcal/mol), relative to anti-u-3' = 0.0 kcal mol⁻¹.

of six pairs of enantiomers (*E-u-syn*, *E-l-syn*, *Z-u-syn*, *Z-l-syn*, *E-anti*, and *Z-anti*) are conceivable. It is noted that excitation of the two rotamers of both diastereomeric precursors (*l*, *u*) can potentially lead to the formation of one (and only one) enantiomer of each rotameric triplet state diastereomer.²⁹ Scheme 6 shows reaction pathways leading from the *anti*-rotamers of triplet **3'** to the triplet states of the fulvene–diyl diradicals **14'**.

Our calculations indicate that the activation enthalpies for the *syn-anti* conversion of the triplet excited states of the two diastereomers of **3'** are somewhat smaller than the activation enthalpies of a smaller system studied by us earlier (R = Me instead of diphenylcyclopropyl).⁶ With ΔH^\ddagger of the order of 10 kcal mol⁻¹ and ΔS^\ddagger of the order of -5 cal mol⁻¹ K⁻¹, *anti-syn* isomerization rate constants of the order of 2×10^4 s⁻¹ can be expected. The activation enthalpies for cyclization of the *syn*-triplet allenes are calculated to be much smaller, of the order of $\Delta H^\ddagger = 3.8$ – 7.6 kcal mol⁻¹. For that reason, the *syn*-triplet allenes, if formed from the *anti*-triplet allenes, will be present in quasistationary concentration only, inaccessible to direct observation. The results obtained by RIMP2/TZVP indicate, however, that a significant portion of triplet allenes can be formed directly as *syn*-rotamer. This population of *syn*-triplet-allenes may be detected by LFP.

It is a priori conceivable that cyclization of the *syn*-allene triplets may initially result in fulvene–diyl-type diradicals that, unlike **14'**, show an *E* configuration at the C=C

SCHEME 7. Possible Interconversion of a Triplet Allene into an *E*-Fulvene Diyl Diradical

(fulvene) bond (Scheme 7). However, steric repulsion between the TIPS group and the diphenylcyclopropyl group (= R) or, in a different rotamer, the triphenylamine moiety, can be expected to exert a strongly destabilizing effect.

Vinyl radicals have been reported to show relatively small barriers for *Z/E*-isomerization³⁰ that are further reduced upon α -silylation.³¹ Even at the primitive UHF/STO-3G level of theory, which in the study by Lalitha and Chandrasekhar resulted in the highest barrier for isomerization of an α -silylvinyl radical,³¹ our attempts to optimize a derivative of **14'** with *E*-configuration at the vinyl radical moiety (*E*-vinyl isomer) were fruitless, resulting in the optimization of the *Z*-silylvinyl isomer instead.³² For that reason we have to assume that (*E*-silyl)fulvene–diyl-type diradicals are no minima on the potential energy hypersurface.

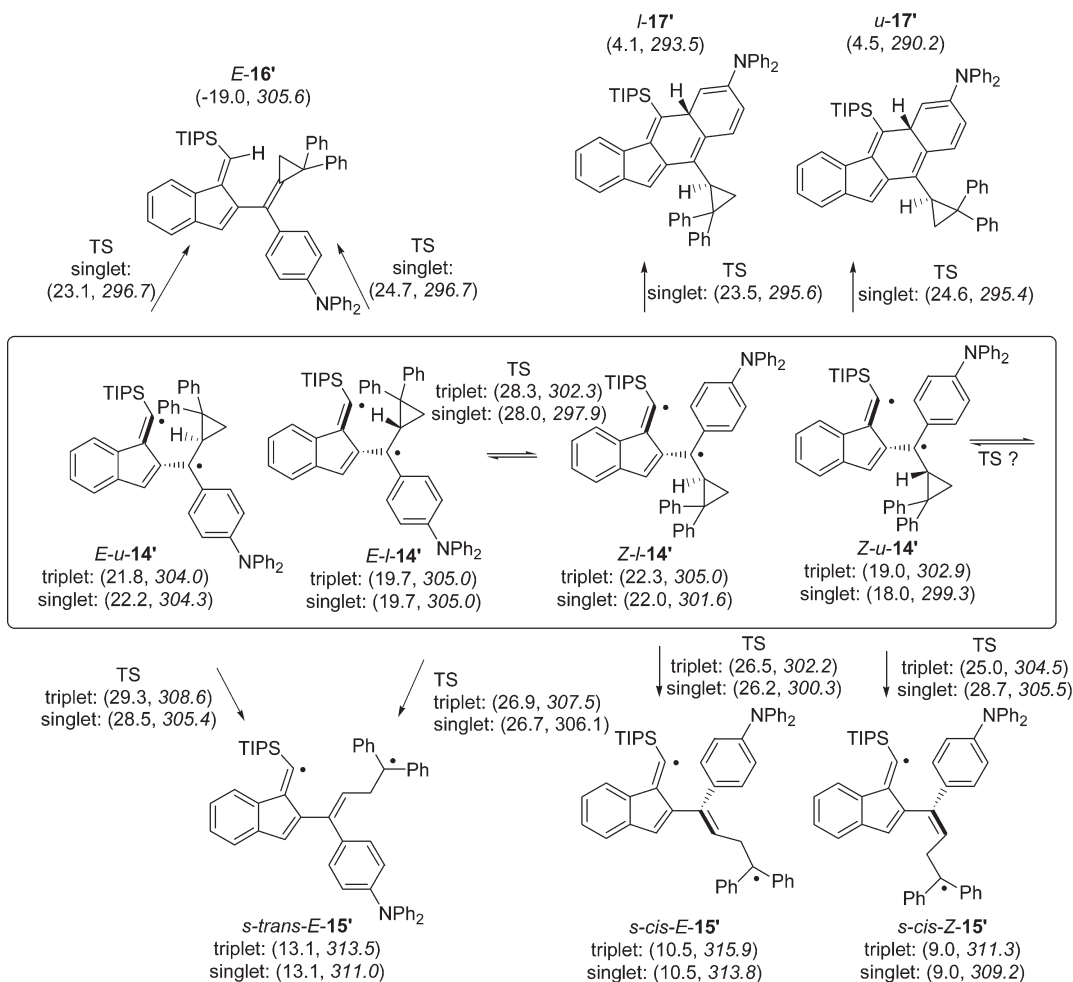
(30) Galli, C.; Guarnieri, A.; Koch, H.; Mencarelli, P.; Rappoport, Z. *J. Org. Chem.* **1997**, *62*, 4072–4077.

(31) Lalitha, S.; Chandrasekhar, J. *Proc. Indian Acad. Sci. (Chem. Sci.)* **1994**, *106*, 259–266.

(32) Attempted optimization at the UB3LYP/6-31G(d) level of theory gave the same result.

(29) Upon excitation, one of the two stereogenic elements present in the molecule (the stereogenic center in the cyclopropane unit) is retained, whereas the stereogenic axis of the linear allene system is converted into other stereogenic elements (helicity, *Z/E*-isomerism).

SCHEME 8. Reaction Pathways Leading from Isomers of Fulvene–Diyl-Type Diradicals **14'** to Ring-Opened Diradicals **15'**, Fulvenes **16'**, and Benzofluorenes **17'**^a



^aIn brackets: enthalpies (in kcal mol⁻¹), relative to anti-*u*-**3'** = 0.0 kcal mol⁻¹. In italics: calculated absolute entropies (in cal mol⁻¹ K⁻¹).

Diradical Reactions. Follow-up reactions of the triplet fulvene–diyl diradicals **14'** include ISC to the singlet state, followed by either hydrogen transfer and fulvene formation (*E*-isomers) or addition to the proximal benzene ring of the triphenylamine moiety (*Z*-isomers). Alternatively, the cyclopropane ring may undergo ring opening, either from the triplet or from the singlet state of **14'**. Scheme 8 shows the results of our calculations on these competing pathways.

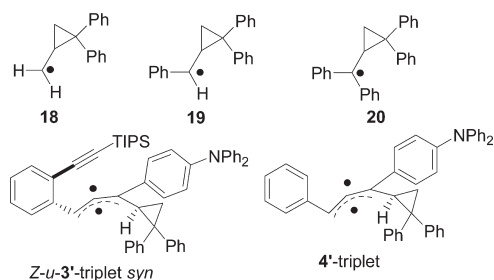
On the basis of the calculated activation enthalpies, the *E*-rotamers of **14'** should preferentially undergo a facile 1,5-hydrogen shift, yielding fulvene **16'**. The calculated activation enthalpies for this strongly exothermic hydrogen shift are very small (of the order of 1–5 kcal mol⁻¹). For that reason, the two diastereomers *E*-**14'** (*l*, *u*) are unlikely to have lifetimes exceeding 1 ns and therefore are not expected to be observed in our experiments. Both diastereomers of *Z*-**14'**, on the other hand, should preferentially undergo intramolecular addition to a benzene ring of the triphenylamine moiety, yielding isomers of **17'**. In contrast, cyclopropylmethyl ring opening of both *E*- and *Z*-**14'** is impeded by a somewhat higher activation enthalpy. Taking into account the calculated entropies, however, the cyclopropylmethyl ring opening may become competitive, as it is much more

favorable in terms of entropy than the hydrogen shift or addition reactions. A difference in activation entropy $\Delta\Delta S^\ddagger = 10$ cal mol⁻¹ K⁻¹ between hydrogen transfer or benzofluorene formation on one hand and ring opening on the other hand translates into a difference of free energy of activation $\Delta\Delta G^\ddagger = 3$ kcal mol⁻¹, which may easily outbalance the relatively small preference for hydrogen transfer or benzofluorene formation in terms of ΔH^\ddagger . This at least applies to *E*-**14'** and *Z*-**14'**, where the calculated activation enthalpies for hydrogen transfer (*E*-**14'**) or addition (*Z*-**14'**) are of the order of 5–6 kcal mol⁻¹. Finally, interconversion of the *Z*- and *E*-isomers of **14'** is also conceivable, with activation enthalpies around 6–8 kcal mol⁻¹.³³

The spin density at the cyclopropylmethyl–carbon atom can be expected to be a crucial factor determining the ease of ring opening. To gain an understanding for the surprisingly high barriers for cyclopropylmethyl ring opening in **14'**, we additionally calculated the activation enthalpies for ring opening of three simple diphenylcyclopropylmethyl radicals, namely the parent diphenylcyclopropylmethyl

(33) We have been unable to localize the transition state linking *Z*-**14'** and *E*-**14'**.

CHART 2. Various Cyclopropylmethyl Radicals



(18), (*E*-diphenylcyclopropyl)phenylmethyl (19), and (diphenylcyclopropyl)diphenylmethyl (20). As the triplet alkenes of importance investigated in this study also bear spin density at the cyclopropylmethyl–carbon atom (and may thus in principle also undergo ring opening), *Z*-*u*-triplet 3' *syn* and triplet 4' were also included in the comparison (Chart 2).

Figure 4 shows a plot of activation enthalpy vs. spin density (for the data, please see Table S1 in the SI). It clearly demonstrates the correlation between the two parameters. The data also indicate that due to a relatively low spin density at the cyclopropylmethyl carbon atom, the cyclopropylmethyl ring-opening reactions in the derivatives investigated by us (14, triplet-4, and triplet-3) are expected to be slower than originally anticipated, and that the lifetimes for these processes may reach well into the nanosecond or even microsecond realm.

Fate of the Ring-Opened Diradicals. Hydrogen transfer in 15', yielding butadiene 6', requires *Z*-configuration at the newly formed carbon–carbon double bond. Among the ring-opened diradicals 15' formed in the cyclopropylmethyl ring-opening reactions of isomers of 14', only *s-cis-Z-15'* matches this requirement. We have been able to locate the transition state for formation of 6' on the singlet hypersurface (Scheme 9). The calculations indicate that the hydrogen transfer requires an activation enthalpy of the order of 10 kcal mol⁻¹, which should bring this process into the low microsecond time domain.

It is noteworthy that *s-cis-Z-15'* is formed by ring opening of *Z-u-14'*, which is the energetically lowest lying fulvene–diyl-type diradical studied, and which also is the diradical least likely to undergo an extremely facile hydrogen shift or addition reaction. For that reason, the hydrogen abstraction mechanism depicted in Scheme 9 appears plausible to us.

Assignment of the Transients Observed. The spectra and behavior of the transients, the results of the product studies, and the calculations allow us to make a reasonable assignment of the transient species observed in the LFP experiments (cf. Scheme 10). Transient D (stable on the ms time scale, formed with a rate constant $k = (1.0 \pm 0.1) \times 10^6 \text{ s}^{-1}$) has already been assigned to butadiene 6 based on its UV/vis spectrum. The discussion above strongly suggests that transient C, which is the direct precursor to D (= 6), should be assigned to *Z-15*, as none of the other isomers of 15 is suitable for hydrogen transfer. The sharp absorption band observed at $\lambda_{\text{max}} = 332 \text{ nm}$ is strongly suggestive of a diphenylmethyl radical moiety.²⁷ As mentioned above, a calculated activation enthalpy of 10.2 kcal mol⁻¹ is consistent with a lifetime of the order of 1 μs . *E*-Isomers of 15 are predicted to be less stable, which would offer an explanation for the fact that we

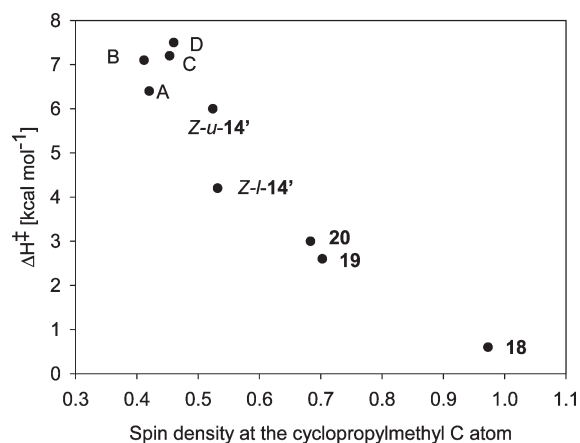
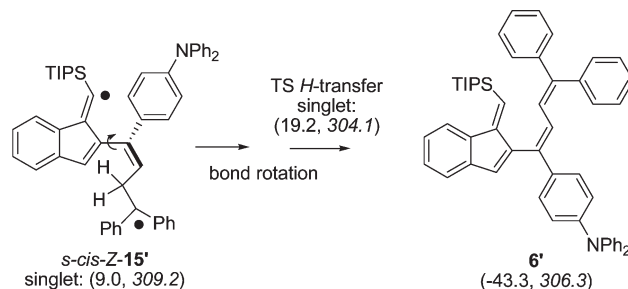


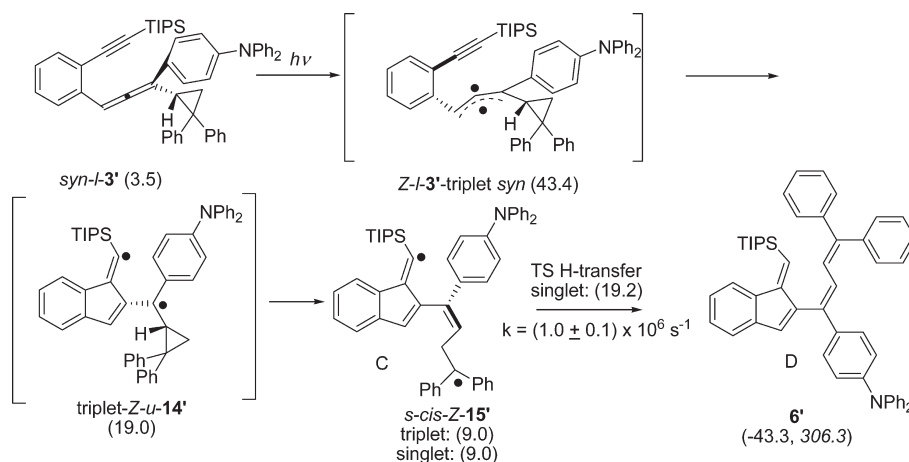
FIGURE 4. Plot of the calculated activation enthalpy for the cyclopropylmethyl ring-opening reaction of a series of 1,1-diphenylcyclopropanes vs. the calculated Mulliken spin density at the cyclopropylmethyl carbon atom: (A) *Z*-*u*-triplet 3' *syn*; (B) triplet 4'; (C) *E*-*l*-14'; and (D) *E*-*u*-14'.

SCHEME 9. Possible Reaction Pathway Leading to 6' from *s-cis-Z-15'*^a

^aIn brackets: calculated enthalpies (in kcal mol⁻¹, relative to anti-*u*-3' = 0.0 kcal mol⁻¹); in italics: calculated absolute entropies (in cal mol⁻¹ K⁻¹).

observe none of them. Moreover, the reactions competing with their formation (formation of ene or Diels–Alder products) are predicted to occur via very small barriers.

Transients A and B are more difficult to assign unambiguously. A ($\lambda_{\text{max}} = 458 \text{ nm}$, $k_{\text{decay}} = (2.3 \pm 0.5) \times 10^6 \text{ s}^{-1}$, quenched by oxygen) likely corresponds to a precursor triplet excited state, possibly the triplet conformer *E*-3-triplet *anti*. Due to a lack of reactivity toward oxygen, transient B ($\lambda_{\text{max}} = 458 \text{ nm}$, $k_{\text{decay}} = (3.4 \pm 0.8) \times 10^5 \text{ s}^{-1}$) is unlikely to correspond to a triplet excited state. Our calculations indicate that the fulvene–diyl-type diradicals 14 may actually have singlet ground states by a very small margin. In previous LFP studies of related allene precursors, transients with characteristics similar to B were assigned to triplet fulvene–diyl-type diradicals.^{4,6} Nevertheless, we hesitate to give an assignment of B to any stereoisomer of 14, as these (singlet) diradicals are predicted to undergo follow-up reactions far too easily to have a lifetime in excess of 1 μs . Moreover, as mentioned above, *Z*-*u*-14 is expected to be the most stable isomer of 14. This species probably is the (invisible) precursor to C. As B is not a precursor to C, an assignment of B to singlet *Z*-*u*-14 can thus be ruled out. What possible assignments remain for B? Ground state triplet fulvene–diyl diradicals can be expected to be longer lived than their counterparts on the singlet spin manifold, as the triplet–singlet energy gap would additionally have to be

SCHEME 10. Possible Reaction Pathway Leading to **6'** from *syn*-**1-3'**

overcome. We cannot rule out the possibility of our calculations giving an inaccurate picture of the potential energy hypersurface and wrongly predicting the stereoisomers of **14** to be ground state singlet species. In this case, an assignment of **B** to a stereoisomer of triplet-**14** would represent a straightforward solution to the problem.³⁴ The lack of reactivity of **B** toward oxygen need not be of concern here, as a related, sterically less congested triplet fulvene–diyl diradical has previously been shown not to react with oxygen, either.⁶

An additional experiment to probe the course of reaction is to compare the intramolecular kinetic isotope effect (KIE) in the thermal and photochemical cyclization of **5**. Recently, we learned that the intramolecular KIE of C²–C⁶ cyclization of enyne–allenes has a meaningful signature with regard to the mechanism.²¹ Hence, it is interesting to see that in both the thermal and photochemical cyclization, the intramolecular KIE is around 1.00. Using our understanding of intramolecular KIE,²¹ this is strong evidence for (i) having basically the same intermediate involved in the hydrogen transfer step for both reaction protocols and (ii) for having a stepwise reaction mechanism with dynamic effect about the diradical.³⁵ As the intermediacy of a singlet diradical is reasonably well established for the thermal pathway by a multitude of mechanistic and computational studies,³⁶ these results suggest that a singlet diradical is involved equally in the final H-transfer in the photochemical process and most likely also in the ring opening of the cyclopropyl radical clock.

Conclusions

The present investigation reveals interesting new details of the mechanism of the photochemical C²–C⁶ cyclization of

enyne–allenes. The reaction sequence is started with excitation of the allene moiety to its triplet state thus igniting C²–C⁶ cyclization to furnish a fulvene–diyl diradical. The intermediacy of the diradical can be derived indirectly from the time-resolved detection of a radical clock derived ring-opened product showing a diphenylmethyl radical functionality (characteristic sharp signal at $\lambda_{\text{max}} = 332 \text{ nm}$). Computational results indicate that radical clock opening in the fulvene–diyl diradical is much slower than that in monoradicals. The investigation, however, failed to provide an experimental kinetic analysis of the ring opening of the singlet fulvene–diyl diradical, as the visible transient **B** was not a direct precursor of **C**.

Experimental Section

General Procedure for the Photochemical Cyclization. The reaction mixture of enyne–allene and 1,4-cyclohexadiene (CHD) (200-fold excess) in dry degassed toluene was irradiated at 300 nm in an inert atmosphere. The reaction progress was monitored by TLC. The product mixture was concentrated and purified with preparative TLC (aluminum sheet, silica gel 60F₂₅₄, *n*-pentane). For characterization of compounds **6**, **7**, **9**, and **10**, see ref 17.

Physical Measurements. For all ¹H and ¹³C NMR spectra chemical shifts refer to the residual protio solvent signals (CDCl₃ 7.26 and 77.0 ppm, C₆D₆ 7.15). Laser flash photolysis: The system employed has already been described.³⁷ Enyne–allene **3** was excited with use of the third harmonic ($\lambda = 355 \text{ nm}$) of a Nd:YAG laser (130 mJ/pulse, 7 ns pulse duration). The concentration of **3** was ca. $3.5 \times 10^{-5} \text{ M}$ in cyclohexane. A flow cell was used to avoid buildup of photoproducts. Prior to experiments, the solutions were purged with argon for ca. 20 min. In oxygen quenching studies, variable mixtures of O₂ with Ar were obtained with use of mass flow controllers (MKS).

Calculations. Geometry optimizations were performed at the (U)B3LYP level of theory,³⁸ using a 6-31G(d) basis.³⁹ The DFT calculations were performed employing the Gaussian03 suite of programs.⁴⁰ RIMP2 single point energy calculations⁴¹ with a TZVP⁴²

(34) We note, however, that a series of calculations on model systems has indicated the B3LYP method to overestimate rather than to underestimate the stability of the triplet state of fulvene–diyls,⁶ and therefore the identity of **B** cannot be regarded as fully settled. An alternative scenario would involve the formation of a phenylvinylcarbene by aryl shift of the singlet excited allene. While such reactions do occur in arylallene photochemistry, they generally have a very low quantum yield.^{27b} As we have not isolated any products indicative of such chemistry, we do not want to embark on any speculations in this direction at this point.

(35) Bekele, T.; Christian, C. F.; Lipton, M. A.; Singleton, D. A. *J. Am. Chem. Soc.* **2005**, *127*, 9216–9223.

(36) (a) Wenthold, P. G.; Lipton, M. A. *J. Am. Chem. Soc.* **2000**, *112*, 9265. (b) Musch, P. W.; Engels, B. *J. Am. Chem. Soc.* **2001**, *123*, 5557. (c) Stahl, F.; Moran, D.; Schleyer, P. R.; Prall, M.; Schreiner, P. R. *J. Org. Chem.* **2002**, *67*, 1453. (d) Schreiner, P. R.; Navarro-Vázquez, A.; Prall, M. *Acc. Chem. Res.* **2005**, *38*, 29–37.

(37) Bucher, G. *Eur. J. Org. Chem.* **2001**, 2463–2475.

(38) Becke, A. D. *J. Chem. Phys.* **1993**, *98*, 5648–5652.

(39) Ditchfield, R.; Hehre, W. J.; Pople, J. A. *J. Chem. Phys.* **1971**, *54*, 724–728.

(40) Frisch, M. J. et al., *Gaussian 03*, Revision C02; Gaussian, Inc., Wallingford, CT, 2004.

(41) Weigend, F.; Häser, M. *Theor. Chem. Acc.* **1997**, *97*, 331–340.

(42) Weigend, F.; Ahlrichs, R. *Phys. Chem. Chem. Phys.* **2005**, *7*, 3297–3305.

basis set were performed with Turbomole software.⁴³ The DFT enthalpies given are corrected for zero-point vibrational energy.

4-Bromo-*N*-(4-bromophenyl)-*N*-{4-[(1*E*)-1-[(1*E*)-1-[(triisopropylsilyl)methylene]-1*H*-inden-2-yl]-4,4-diphenylbuta-1,3-dienyl-phenyl]benzenamine (6):¹⁷ IR (film) 3051 (m), 2942 (s, C–H), 2865 (s), 1582 (m), 1486 (s), 1312 (s), 1265 (s), 1178 (w), 1072 (m), 1008 (m), 882 (m), 823 (s), 740 (s), 702 (s) cm⁻¹; HRMS calcd for C₃₃H₂₇⁸¹Br⁷⁹BrN 889.215, found 889.215.

1st isomer: yield 7.7 mg; ¹H NMR (400 MHz, C₆D₆) δ 1.03 (d, *J* = 7.4 Hz, 18H), 1.32 (septet, *J* = 7.4 Hz, 3H), 6.52 (d, *J* = 8.8 Hz, 4H), 6.60 (d, *J* = 8.7 Hz, 2H), 6.69 (s, 1H), 6.83 (s, 1H), 6.90–6.93 (m, 3H), 7.10 (d, *J* = 8.8 Hz, 4H), 7.12–7.16 (m, 3H), 7.16–7.24 (m, 8H), 7.30 (d, *J* = 11.5 Hz, 1H), 7.37 (d, *J* = 6.9 Hz, 2H), 7.94 (dd, *J* = 5.4, 2.7 Hz, 1H); ¹³C NMR (100 MHz, CDCl₃) δ 12.9, 19.1, 115.6, 120.9, 122.2, 123.7, 125.0, 125.5, 126.4, 127.3, 127.4, 127.6, 127.7, 127.9, 128.1, 128.2, 130.7, 132.3, 132.7, 133.5, 136.2, 137.2, 137.7, 139.9, 142.3, 142.7, 143.3, 143.9, 145.9, 146.2, 155.4 ppm.

2nd isomer:²⁴ yield 7.7 mg; ¹H NMR (400 MHz, CDCl₃) δ 0.98 (d, *J* = 7.4 Hz, 18H), 1.29 (m, 3H), 6.28 (s, 1H), 6.53 (d, *J* = 11.6 Hz, 1H), 6.68 (s, 1H), 6.97 (d, *J* = 8.8 Hz, 4H), 7.00 (d, *J* = 8.6 Hz, 2H), 7.01 (d, *J* = 11.7 Hz, 1H), 7.08–7.12 (m, 1H), 7.21–7.30 (m, 14H), 7.35 (d, *J* = 8.8 Hz, 4H), 7.59 (d, *J* = 7.6 Hz, 1H); ¹³C NMR (100 MHz, CDCl₃) δ 12.9, 19.1, 115.8, 120.6, 122.1, 123.0, 124.9, 125.5, 125.8, 127.4, 127.5, 127.8, 128.2, 128.8, 130.6, 131.0, 131.2, 132.4, 133.4, 135.6, 136.8, 137.9, 139.7, 142.7, 143.3, 144.1, 146.0, 146.2, 146.7, 154.8 ppm.

4-Bromo-*N*-(4-bromophenyl)-*N*-{4-[(1*E*)-1-[(1*E*)-1-[(triisopropylsilyl)methylene]-1*H*-inden-2-yl]-4,4-diphenylbuta-1,3-dienyl-phenyl]benzenamine.

Bis(4-bromophenyl){4-[(1*E*)-1-[(1*E*)-1-[(triisopropylsilyl)methylene]-1*H*-inden-2-yl][(2-phenylcyclopropylidene)methyl-phenyl]benzenamine (8): ¹H NMR (400 MHz, CDCl₃) δ 1.01–1.03 (m, 18H), 1.15–1.21 (m, 2H), 1.31–1.39 (m, 3H), 1.86 (t,

J = 9.1 Hz, 1H), 6.30 (s, 1H), 6.81 (s, 1H), 6.84 (d, *J* = 8.8 Hz, 4H), 6.99 (d, *J* = 8.8 Hz, 2H), 7.04–7.06 (m, 2H), 7.12–7.18 (m, 6H), 7.28 (d, *J* = 9.0 Hz, 4H), 7.36 (d, *J* = 8.8 Hz, 2H), 7.37 (d, *J* = 6.9 Hz, 2H), 7.69 (d, *J* = 7.5 Hz, 1H); MS-EI (70 eV) *m/z* 813.2 (M⁺); HRMS calcd for C₃₃H₂₇⁸¹Br⁷⁹BrN 813.183, found 813.183.

Bis(4-bromophenyl)[10-(2,2-diphenylcyclopropyl)-11,11a-dihydro-4*aH*-benzo[*b*]fluoren-7-yl]amine (11): ¹H NMR (400 MHz, CDCl₃) δ 2.06 (dd, *J* = 9.4, 5.2 Hz, 1H), 2.51 (dd, *J* = 7.0, 5.3 Hz, 1H), 3.37 (dd, *J* = 8.2, 8.2 Hz, 1H), 3.99 (s, 2H), 6.78–6.88 (m, 4H), 6.96 (d, *J* = 8.8 Hz, 4H), 7.11 (dd, *J* = 2.3, 9.2 Hz, 1H), 7.27–7.33 (m, 4H), 7.36 (d, *J* = 8.8 Hz, 4H), 7.41 (d, *J* = 7.3 Hz, 3H), 7.48 (d, *J* = 7.5 Hz, 2H), 7.51 (d, *J* = 7.7 Hz, 1H), 7.76 (d, *J* = 6.8 Hz, 1H), 7.81 (s, 1H), 8.20 (d, *J* = 9.2 Hz, 1H); ¹³C NMR (100 MHz, CDCl₃) δ 18.7, 29.7, 29.9, 36.8, 115.5, 116.5, 120.3, 121.5, 123.2, 124.9, 125.5, 125.7, 126.3, 126.8, 126.9, 127.3, 127.5, 128.2, 128.6, 128.8, 129.7, 130.3, 132.3, 134.3, 140.6, 140.9, 141.2, 143.6, 143.7, 145.9, 146.5 ppm; MS-EI (70 eV) *m/z* 733.1 (M⁺); HRMS calcd for C₄₄H₃₁⁸¹Br⁷⁹BrN 733.081, found 733.080.

Acknowledgment. We are very much indebted to the Deutsche Forschungsgemeinschaft and the Fonds der Chemischen Industrie for support of our research. Work performed in Glasgow was supported by the Glasgow Centre for Physical Organic Chemistry as funded by the EPSRC. G.B. is grateful for this support. This publication is dedicated to Prof. Dr. C. Rüchardt on the occasion of his 80th birthday.

Supporting Information Available: Experimental procedures for compounds **4**, **5**, **12H**, **12D**, and **13**, ¹H, ¹³C, and HRMS spectra for all compounds, LFP results; and details of the computation. This material is available free of charge via the Internet at <http://pubs.acs.org>.

(43) TURBOMOLE V5-9-1, University of Karlsruhe, 2007.